Journal of Crystal Growth 41 (1977) 5–12

FLAME-FUSION GROWTH OF $SrTiO_3$

J.G. BEDNORZ * and H.J. SCHEEL
IBM Zurich Research Laboratory, 8803 Rüschlikon, Switzerland

Received 3 January 1977; revised manuscript received 5 June 1977

Exact growth conditions for reproducible production of $SrTiO_3$ crystals of optical quality by the flame-fusion method have been defined. The overflow problem could be solved by precise adjustment of the $SrCO_3$ excess in the starting powder to the SrO evaporation. The thickness of the molten layer is nonuniform and varies from 0.4 mm in the center to 1.4 mm at the periphery. The crystals are characterized by their dislocation densities, lattice constant and EPR spectra.

1. Introduction

Strontium titanate at room temperature is cubic (perovskite, Pm3m) and transforms below a range of 105 to 99 K to a nonferroelectric tetragonal phase (I4/mcm). This second-order phase transition [1] as well as interesting electrical and optical properties initiated systematic physical studies on $SrTiO_3$. The optical similarity with diamond (index of refraction 2.4, optical dispersion 0.1) resulted in commercial flame-fusion growth of this synthetic gem "fabulite" by two companies [2].

The patents [3] and publications [4–6] do not contain all the necessary data on the experimental conditions for growth of large $SrTiO_3$ crystals. Therefore, a systematic investigation on the flame-fusion growth process of $SrTiO_3$ was undertaken in order to evaluate the conditions required in the growth of large crack-free crystals. Recently, the structural perfection of $SrTiO_3$ grown by various techniques has been related to the growth conditions and several characterization data on the flame-fusion-grown crystals described in this paper have been published [7,8].

2. Experimental

The versatile flame-fusion apparatus used for the present work will be described elsewhere [9]. Here, only specific details in connection with $SrTiO_3$ are discussed. The design of the three-tube burner is very similar to that of Linz et al. [5] although Nakazumi [6] applied a simple double-tube burner for $SrTiO_3$. The crystal was growing in the center of an alumina tube of 4 cm internal diameter which was positioned in the afterheater. The latter was heated only after the growth run for in-situ annealing of the grown crystals.

The temperature profile of the flame with the conditions applied for growth of $SrTiO_3$ has been measured inside the apparatus by optical pyrometry. The temperatures of the five saw teeth (facing upward) of a vertical ZrO_2 ceramic plate ($20 \times 20 \times 2$ mm) were measured in the center of the tube as a function of the distance from the burner. The emissivity of the coarse ZrO_2 ceramic was determined as 0.75 (compared to 0.18–0.43 published for dense ZrO_2) and the temperatures corrected accordingly. The resulting temperature profile shown in fig. 1 indicates that the flame temperatures are significantly higher than the melting point of $SrTiO_3$ ($1920 \pm 15°C$, as determined by DTA). These high flame temperatures might be the reason for the high melting points of $SrTiO_3$ reported earlier (2050°C [5], about 2050 to 2100°C [3], 2080–2130°C [4a]). Systematic flame and wall temperature profiles have been measured by Khambatta et al. [10] who tried to relate the data to their thermal model which we have not yet applied to $SrTiO_3$.

The preparation of $SrTiO_3$ feed powder with

---

* Present address: Laboratorium für Festkörperphysik, ETH, 8093 Zürich, Switzerland.

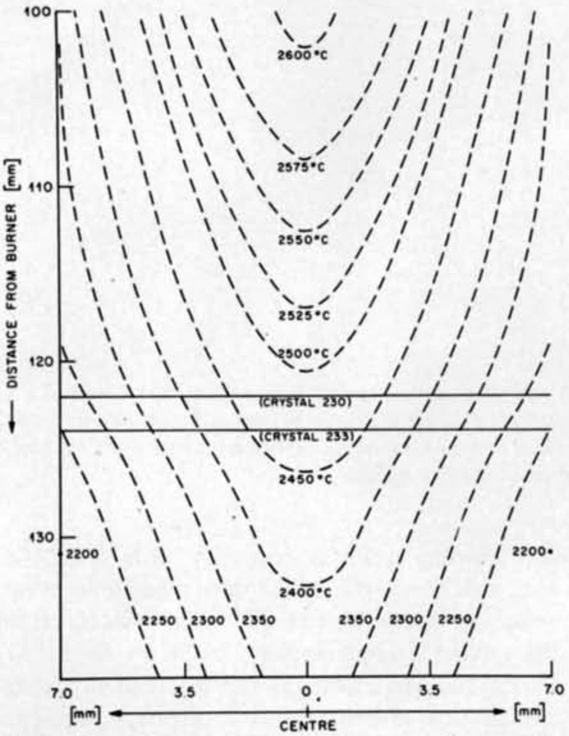

Fig. 1. Temperature profile for the flame conditions used for growth of $SrTiO_3$ crystals nos. 230 and 233 (their positions are indicated by horizontal lines). The precision of the measured temperatures is ±10°C, the estimated accuracy ±30°.

suitable flow characteristics for flame-fusion growth is rather critical. Powders of grain size 0.05–0.125 mm for the present investigation were supplied by Nakazumi [2] (for crystals nos. 230, 232 and 233) or prepared [11] following a recipe of Merker [4a] modified by Linz et al. [5] and by Foguel [12]. The excess $SrCO_3$ required (see section 3) was monitored by chemical analyses [11]. The mesh width of the sieve used in the Verneuil apparatus varied from 0.15 to 0.18 mm (80–100 mesh).

Following normal flame-fusion growth practice established by Verneuil about 80 years ago, a $SrTiO_3$ sintered cone of about 10 mm length was formed before the temperature was raised in order to get a small melt droplet at the top of the cone. Then a thin neck of at least 6 mm length was initiated, and finally, the diameter of the growing crystal was increased (compare fig. 8 of section 4). The powder falls onto the molten cap of the growing crystal which is lowered in order to remain in the hot region of the hydrogen–oxygen flame.

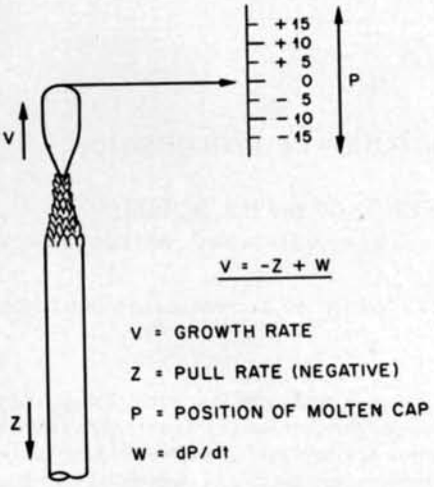

Fig. 2. Relation between the measured position p of the molten cap, the adjustable pull rate z and the resulting growth rate v.

The position of the top of the crystal was measured by an optical system [9]. The relation of this position p (and of the related velocity $w = dp/dt$) to the growth rate v and to the adjustable pull rate z is demonstrated in fig. 2. The starting position for the top of the pull rod is given by $p = 0$. [The distance to the burner at this time is $d_0 = 109$ mm or 106 mm for nos. 230 and 233 (see fig. 1), respectively. During the experiment, the distance from the burner to the molten cap is given by $d = d_0 - p$.] The growth rate could be determined for all growth phases according to $v = -z + w$.

The variation with time of the parameters p, w, z and v during experiment no. 233, and their effect on the dimensions of the growing crystal are plotted in fig. 3. In the first 20 min after the melt–droplet formation, the crystal neck grew with a high rate v of about 80 mm h^{-1} which was partially compensated by adjusting the pull rate z. After about half an hour a steady state was reached by adjusting the growth rate to a value of 17 ± 4 mm h^{-1}.

The increase of diameter and length of the growing crystal is plotted in the lower part of the diagram. Also included in fig. 3 are the flow rates of hydrogen and of the central oxygen which are increased during this experiment in order to increase the crystal diam-

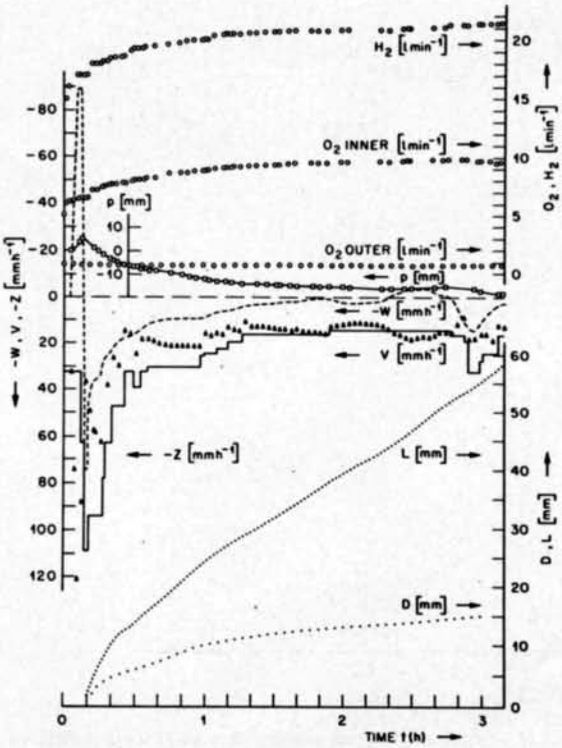

Fig. 3. Change of the growth parameters during an experiment (no. 233): (○) flow rate of H_2 and O_2 (ℓ min^{-1}); (□) position p of the molten cap of crystal (height difference from a reference 106 mm below burner); (– – –) variation of p with time $-w$ (mm h^{-1}); (△) crystal growth rate v (mm h^{-1}); (———) pull rate $-z$ (mm h^{-1}); (· · · · · ·) length L and diameter D of the growing crystal (mm).

eter, whereas the outer oxygen flow is kept constant. Previously [4a] a strongly reducing flame with $H_2 : O_2$ ratios of 5 : 1 to 10 : 1 was thought to be necessary for the growth of $SrTiO_3$. In the present experiments a slightly reducing flame proved to be satisfactory and at the same time prevented hydrogen explosions. Gorina et al. [4c] even suggested oxidizing flame conditions.

3. The overflow problem

In the first experiments, overflow of the molten cap was always observed when the growing crystal had reached a certain size, even when various amounts of excess SrO in the feed powder for compensation of the SrO evaporation losses were used. It became evident that the evaporation loss of SrO during the growth process had to be precisely compensated in order to prevent overflow. When the excess SrO in the powder was insufficient, the melt became enriched with TiO_2. This produces a reduction of the liquidus temperature, as can be seen in the $SrO-TiO_2$ phase diagram [13], and results in overflow in the unchanged flame. Similarly, a too large excess of SrO leads to overflow by enrichment in SrO-rich titanates. This was proven by X-ray photographs taken with a focussing Guinier–De Wolff camera of the overflowed material: in the cases of insufficient SrO excess, TiO_2 (rutile) lines were found (ASTM 4-0551), and when the SrO excess was too large, the diffraction lines of Sr_2TiO_4 (ASTM 24-1243) and of $Sr_3Ti_2O_7$ (ASTM 11-663) were identified.

The results of X-ray analyses of the overflowed material from several crystals with various average growth rates and with various amounts of SrO excess (expressed in weight % $SrCO_3$) are shown in fig. 4. Overflow was observed in the regions of too large $SrCO_3$ excess and of too small $SrCO_3$ excess (=TiO_2 excess in the overflowed material). Large crystals (nos. 230, 233, 235, 237 and a number of doped crystals) could only be grown at the boundary of these two regions, and average growth rates between 17 and 24 mm h^{-1} were applied for the large crystals obtained. These favourable growth conditions were established for our system and flame conditions. In other systems the critical composition range may shift somewhat. However, the range of 0.1 to 20% SrO claimed to be suitable by Merker [3] seems to be too wide. The range of Linz et al. [5] of 1 to 3 wt% SrO is more realistic. According to our experience the TiO_2 excess of about 3% reported by Gorina and Maksimova [4c] would not result in large crystals.

Under specific conditions such as very high gas-flow rates, crystals with too small SrO excess could be grown up to about 1 cm length without overflow (nos. 221, 223 and 224). The explanation for this behaviour was that the excess TiO_2 had crystallized in a 1 to 2 mm layer at the periphery of the crystal under conditions of constitutional supercooling. The temperature gradient in the centre of the boule was higher than at the periphery thus allowing local stable growth. The surfaces of the molten caps in these special cases showed a smaller radius than usual and thus

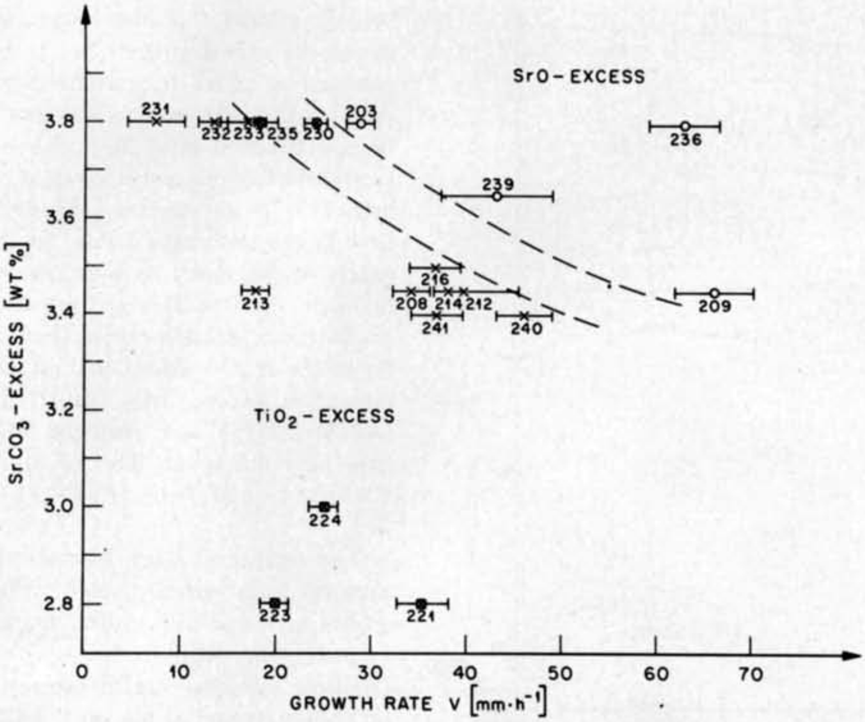

Fig. 4. X-ray results of the overflowed molten caps in relation to $SrCO_3$ excess in the feed powders versus average growth rate. Large $SrTiO_3$ crystals can presumably only be grown in a narrow range between SrO excess in the melt (○) and TiO_2 excess (×). An upper limit to this range is indicated by the two dashed lines. Crystals with a composite $SrTiO_3$–TiO_2 skin are marked by ■.

favoured the flow of the TiO_2-rich melt to the periphery. There, the small temperature gradient initiated instability at the growing-crystal interface which resulted in inclusions with eutectic structure as shown in fig. 5a. An inclusion corresponding to the section indicated in the photograph was examined by scanning electron microscopy and is shown in fig. 5b, where the TiO_2 and $SrTiO_3$ regions are clearly distinguished in the picture taken from back-scattered electrons. Energy-dispersive X-ray analyses of regions I and II marked in fig. 5b indicated the presence of $SrTiO_3$ (I) in a TiO_2-rich matrix (II) as shown in fig. 5c. The Fe lines originated from back-scattered electrons striking the pole shoe material.

The SrO excess versus growth-rate relationship shown in fig. 4 seems to indicate that at low growth rates SrO evaporation from the molten cap becomes significant, whereas at high growth rates, the constant evaporation of SrO from the large surface of the powder (or of the droplets) in the flame is approached. However, more systematic work is required for a quantitative discussion of the SrO evaporation, especially since the hydrogen-oxygen ratio of the flame will also affect the evaporation rate.

4. Crystal-growth results

Reproducible growth of crack- and inclusion-free $SrTiO_3$ crystals up to 15 mm diameter and 30 mm length was achieved when the 3.8 wt% excess of $SrCO_3$ was used in the feed material in combination with growth rates between 17 and 24 mm h^{-1}. Examples of crystals grown from high-purity powder of Nakazumi (nos. 230 and 233) and grown from powder prepared [11] from analytical-grade chemicals (nos. 235 and 237) are shown in fig. 6. The two former crystals are (after an annealing procedure of about 15 h at 500–1200°C in oxidizing atmosphere) colourless to the eye; the latter are light yellow when kept in the dark or when heated up to 100°C, and become dark brown under the influence of light. This

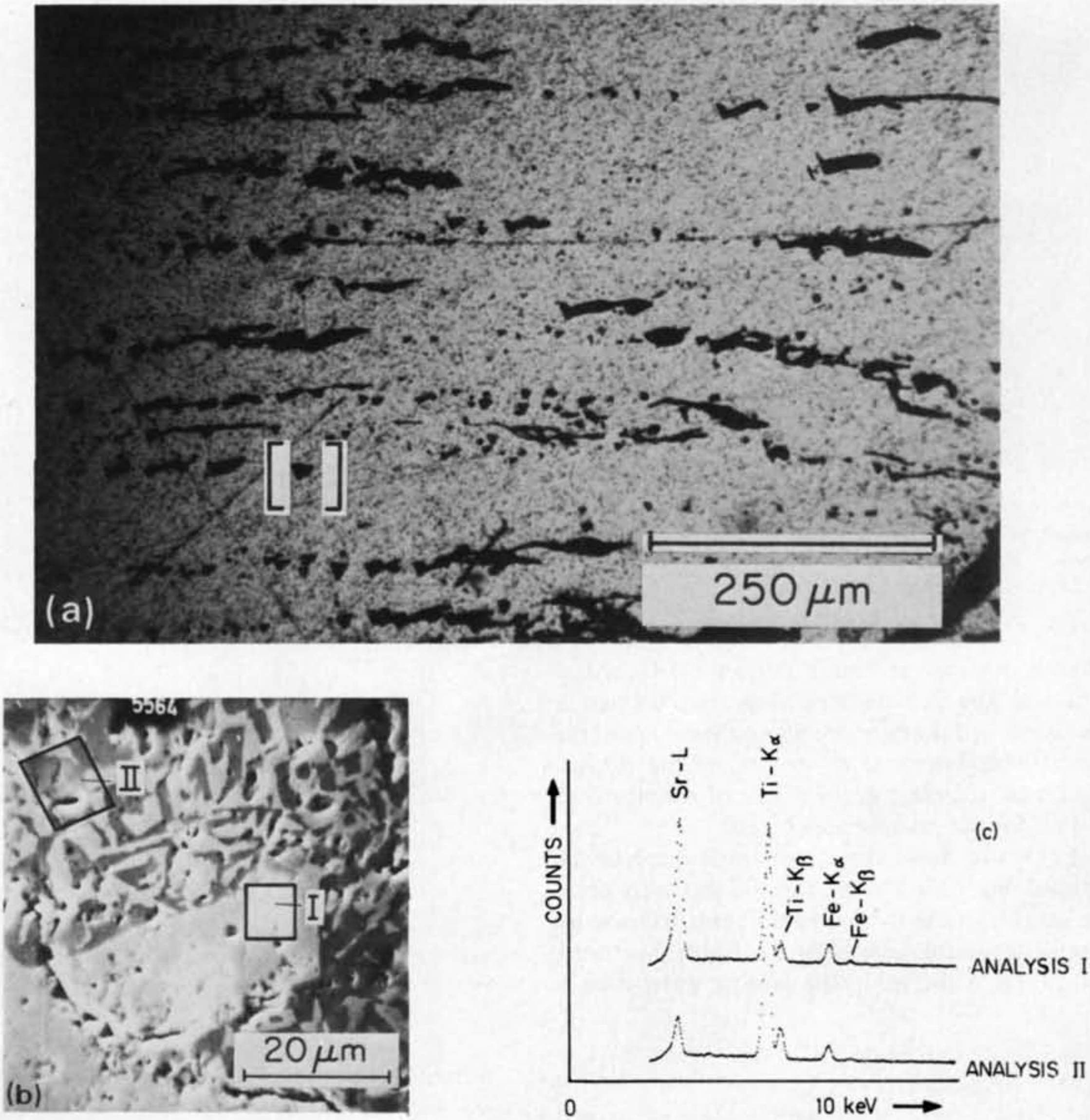

Fig. 5. (a) TiO_2-rich inclusions in the skin of a crystal grown from feed powder with too low (in this case 1.4 wt%) $SrCO_3$ excess; (b) SEM photograph of an inclusion as marked in fig. 5a; (c) X-ray fluorescence lines of the two positions I and II indicated in (b).

reversible effect has been described earlier [14] for photochromic or "thermochromic" $SrTiO_3$. In our case, Fe^{3+} and Cr^{3+} in amounts of about 50 ppm have been found by EPR [15], whereas colourless crystals contain only a few ppm of Fe^{3+} as shown in the EPR spectrum in fig. 7. The optical absorption spectra in the visible and infrared ranges have recently been discussed [7,8].

In contrast with other flame-fusion-grown crystals the thickness of the molten layer at the top of the growing $SrTiO_3$ crystals could be determined very precisely. After shut-off of the flame the molten cap solidified as a polycrystalline crust, which at room temperature could easily be removed by tapping off, thus allowing the measurement of the locally-varying cap thickness. The result is demonstrated in fig 8

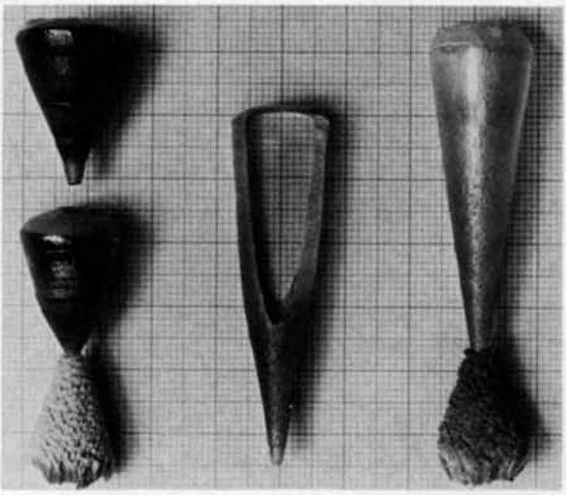

Fig. 6. Examples of crystals grown from analytical-grade powder (left, nos. 235and 237) and of highly-purified $SrTiO_3$ powder (right, nos. 230 and 233) [mm scale]. Crystal 230 has been polished.

where a cross-section through a typical $SrTiO_3$ crystal is shown. The melt thickness varies from 0.4 mm in the centre to 1.4 mm above the peripheral rim of the crystal–melt interface. An analysis of the thermal conditions according to the model of Khambatta et al. [10] has not yet been undertaken.

Fig. 8 also shows the characteristic shape of the crystals: the narrow neck, the constant increase of the diameter up to the desired thickness, followed by a continuing small increase of the diameter until the end of the experiment. The primary sinter cone is formed before crystallization of the neck is initiated; the final sinter cone grows during the formation of the neck.

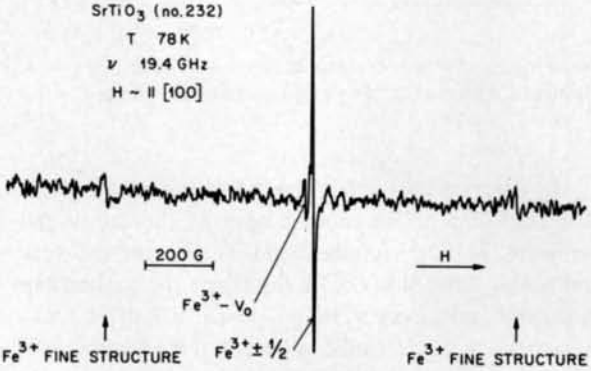

Fig. 7. EPR of a high-purity $SrTiO_3$ crystal (no. 232) at liquid-nitrogen temperature showing a few ppm of iron.

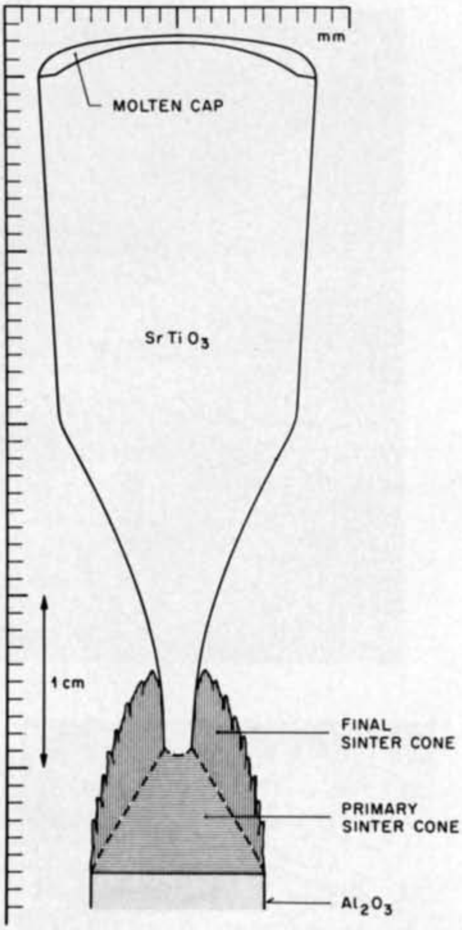

Fig. 8. Cross-section of a typical crystal showing the nonuniform thickness of the molten cap, the ideal crystal shape, and the sintered cones.

Linz et al. [5] described a preferred orientation along the [110] direction when the crystals grow from a sintered cone. However, we did not find this effect. As shown in fig. 9, the orientations of the growth directions of our self-nucleated crystals are spread over the whole section of the stereographic projection, and thus do not indicate a preferred orientation which, if at all, would be expected along the [111] direction.

The lattice constant was determined from X-ray powder-diffraction photographs obtained with a

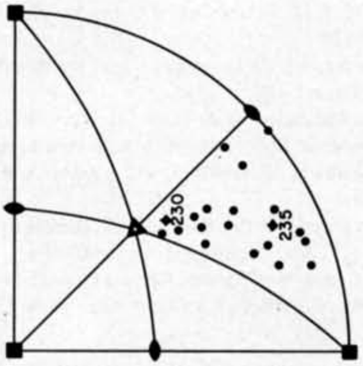

Fig. 9. Section of a sterographic projection of the orientation of the growth directions of 20 crystals as determined from Laue photographs.

focussing Guinier camera of Jagodzinski type using $CuK\alpha_1$ radiation. The lines of $SrTiO_3$ and of 99.999% silicon used as an internal standard were measured and corrected with respect to film shrinkage with the help of a special computer program of Kroll [16]. The refinement of the lattice constant with a least-square program [17] gave $a = 3.9053 \pm 0.0004$ Å, in reasonable agreement with earlier room-temperature data. Higher precision cannot be achieved owing to the linewidth of flame-fusion-grown $SrTiO_3$ crystals of 5–8 min [7].

Dislocation densities of various crystals were determined by etching polished (100) faces with the etchant reported by Waugh et al. [18] (H_2O, HNO_3 HF in the volume ratio 2 : 2 : 1, eight minutes at room temperature). The number of etch pits was determined on a micrograph using a point counter, and the etch-pit density was obtained by taking into account the magnification. Crystals nos. 203, 232 and 235 gave etch-pit densities of $1–4 \times 10^6$ cm^{-2}, and a Nakazumi [2] crystal 5×10^6 cm^{-2}. These values are typical for flame-fusion-grown crystals, and only Nakazumi [6] reported Verneuil-grown $SrTiO_3$ crystals of lower dislocation densities of about 10^4 cm^{-2}. Much lower dislocation densities are obtained by crystallization from high-temperature solutions [19].

5. Conclusions

The main problem in flame-fusion growth of $SrTiO_3$, the overflow of the molten cap, was analyzed. By relating the average growth to the amount of excess $SrCO_3$ in the feed powder, the critical conditions for growth of large $SrTiO_3$ crystals could be determined, and the important growth parameters are described. The thickness of the molten cap is nonuniform and significantly larger than thicknesses reported for alumina and ruby. The thick molten layer allows the application of relatively coarse feed powder of 0.050 to 0.125 mm grain size. The requirement of colourless crystals necessitates additional purification of the starting materials for the feed-powder preparation.

Acknowledgements

Discussions with P. Dill, M. Foguel (†), A Linz, L. Merker and Y. Nakazumi are gratefully acknowledged. Thanks are due to W. Berlinger for taking the EPR spectra and to R. Meili for supplying powders and making chemical analyses. SEM and X-ray fluorescence analysis of the eutectic structure were done in collaboration with R. Blaschke. This work was partially performed in connection with a master's thesis (J.G.B., University of Münster FRG) supported by W. Hoffmann.

References

[1] K.A. Müller, W. Berlinger and F. Waldner, Phys. Rev. Letters 21 (1968) 814.

[2] Nakazumi Crystals Corp., Ikeda-Shi, Osaka-fu, Japan; National Lead, Titanium Division, South Amboy, NJ 00879, USA.

[3] U.S. Patents 2,628,156 (1953); 2,684,910 (1954); 2,723,915 (1955).

[4] (a) L. Merker, Trans. AIME Min. Engng. 202 (1955) 645;
(b) M.D. Beals and L. Merker, Mater. in Design Engng. (January 1960);
(c) Y.I. Gorina and G.V. Maksimova, Growth of Crystals 3 (1962) 326; Y.I. Gorina, A.M. Kashtanova, G.V. Maksimova and G.I. Skanavi, Soviet Phys.-Cryst. 6 (1961) 377;
(d) J.A. Adamski, J. Appl. Phys. 36 (1965) 1784.

[5] A. Linz, E.F. Farrell, M.J. Redman, A. Berkebile and A. Vetrovs, MIT Insul. Lab. Techn. Report 185 (December 1963).

[6] Y. Nakazumi, Bull. Osaka Electrocommun. Univ. Natur. Sci. Series No. 5 (1969), translation obtained from Dr. Y. Nakazumi.